Proceedings of the ASME 2010 3rd Joint US-European Fluids Engineering Summer Meeting and 8th International Conference on Nanochannels, Microchannels, and Minichannels
FEDSM-ICNMM2010
August 1-5, 2010, Montreal, Canada

FEDSM-ICNMM2010-30856

OPTIMIZATION OF DIFFUSER/NOZZLE ELEMENTS FOR RECTIFICATION VALVELESS MICROPUMPS

A. Azarbadegan*, C.A. Cortes-Quiroz, E. Moeendarbary, Ian Eames

Department of Mechanical Engineering
University College London
London, WC1E 7JE, UK
*Correspondence to: s.azarbadegan@ucl.ac.uk

ABSTRACT

There has been a growing interest in understanding the flow behaviour inside diffuser/nozzle elements in order to identify performance characteristics of these elements for micropump applications. Flat-walled diffuser/nozzle element is the most commonly used type for valveless micropump applications due to its ease of fabrication and compact design. In this paper, we study generic flat-walled diffuser/nozzle elements and apply optimization techniques to explore how the pumping efficiency can be improved by changing geometry to provide higher rectification efficiency and lower pressure drop in rectification valveless micropumps. The primary motivation for this study is to evaluate the performance of flat-walled diffuser/nozzle elements based on geometry variations under several Reynolds numbers (Re). In this study we employ a design methodology for diffuser/nozzle elements that incorporates computational fluid dynamics (CFD) within an optimization methodology. To start the process a series of geometric parameters are selected including element neck width, depth, divergence angle, and entrance fillet radius. Then, the pressure drop and rectification property of an element are calculated as performance parameters, i.e., by varying the geometry it is desirable to maximise pressure rise and the rectification property of the element. Design of experiments (DOE) is employed to generate the experimental table which corresponds to different geometries representing the design space. These limited numbers of geometries generated by DOE are evaluated by using CFD to obtain corresponding performance parameters. By preparing all the design and performance parameters, Surrogate model (SM) technique is applied to obtain the relationship (approximation function) between design and performance parameters. Eventually, based on the developed approximation functions or response surfaces, a multi-objective genetic algorithm (MOGA) is employed to maximise pressure rise and rectification property of diffuser/nozzle element. This design methodology is a very powerful tool to design and optimise flat-walled diffuser/nozzle elements for micropump applications and can speed up the micropump design process significantly.

1 INTRODUCTION

It would be less practical to devise a full lap-on-a-chip system unless someone can incorporate miniaturized pump into the microfluidic chip. Valveless micropumps are one of the most robust types of micropump as they are more reliable, less prone to clogging and fatigue, and can operate with biofluids so that they can be easily integrated into different microfluidic systems. One of the main challenges in designing valveless micropumps is to understand the underlying physics of these devices to be able to customise their design. Previous studies have shown the most identifying and central element in valveless micropumps is the rectifying element [1, 2]. In most designs these rectifying elements are diffuser/nozzle elements [1, 3, 4] and in few of them Tesla valves [5, 6] or systems which work based on temperature dependent viscosity [7]. Diffuser/nozzle elements are considered since they show higher rectification efficiencies compared to other two options. Improving the design of these elements can highly improve the performance of micropumps in terms of pressure and flow characteristics which leads to overall enhancement of system.

Despite many experimental, analytical and numerical approaches which are conducted to understand the flow behaviour inside diffuser/nozzle elements for valveless micropumps, there is still a gap in designing procedure of these elements for micropump applications. Computational Fluid Dynamics (CFD) is an alternative way of designing the fluidic

devices that can save both money and time compared to experimental approaches. Furthermore combining CFD with optimization techniques can reduce the computational costs and enables researchers to achieve the best optimized designs. The aim of this study is to employ a design methodology to optimise the diffuser/nozzle elements in valveless micropumps.

In this study we implemented a methodology which was successful in other microfluidic applications such as micromixer design [8-10]. The procedure starts by defining the range of geometrical parameters. For example, the geometry of a diffuser/nozzle element can be parameterised as shown in Figure 1. This figure shows eight geometrical parameters (*W1, W2*, *W3*, *L*, *D*, L_c, *r*, and θ), indeed it should be noted that there are only seven independent parameters. It is clear that all these parameters don't affect the rectification efficiency of the diffuser/nozzle element in the same way. Therefore, a sensitivity analysis is required to limit the number of parameters to reduce the number of calculations. Based on previous studies [11, 12] *W1*, *L*, *D* and θ are the most identifying parameters, but something that is missing in previous studies is the effect of fillet radius, *r*, and width of the diffuser outlet, *W2*, on the efficiency of these elements. The considered parameters in this study are *W1*, *W2*, *D*, and *r*. It should be noted that *W2* is considered as an independent variable which can either be larger or smaller than *W3*. In this study the range of variables are defined in Table 1.

Table 1. Range of geometrical parameters

	Min (μm)	Max(μm)	Fixed (μm)
W1	400	2000	-
W2	600	6000	-
D	50	500	-
r	500	900	-
L	-	-	40000
W3	-	-	4000
Lc	-	-	40100

Another parameter in this study is Reynolds number which is based on the hydraulic diameter of the inlet channel and inlet velocity *U* ($Re=\rho(2DW3/(D+W3))U/\mu$). This Reynolds number varies from 100 to 1000 in increments of 100. The aim of this design methodology is to give us a tool to design the most efficient rectification elements for valveless micropumps. The rectification properties of these elements depend on their pressure drop coefficient values. Pressure drop coefficient is defined as follows:

$$\varsigma = \frac{\Delta P}{\frac{1}{2}\rho u_t^2}, \qquad (1)$$

where u_t is the throat velocity (velocity in the narrowest part of the element) and ΔP is measured along the element length (*L*). Here ς_+ and ς_- are used to show the pressure drop coefficient in diverging and converging directions, respectively. [2] have shown for single chamber micropumps and [10, 13, 14] for double chamber micropumps that the flow rate and pressure rise are proportional to $\varsigma_- - \varsigma_+$ and flow rate is inversely proportional to $\varsigma_- + \varsigma_+$. Therefore, to have a more efficient pump we need to maximise $\varsigma_- - \varsigma_+$ and minimize $\varsigma_- + \varsigma_+$. The detailed design methodology is explained in the following section.

2 METHODOLOGY

The basic diffuser/nozzle element and the geometric dimensions used for parameterization and optimization are shown in Figure 1.

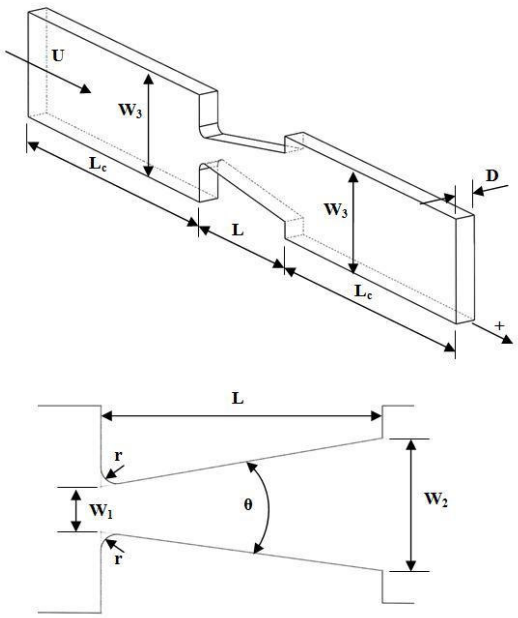

Figure 1. Isometric and top views of a diffuser/nozzle element showing characteristic dimensions and geometric parameters.

For the study of the diffuser/ nozzle element under different operation conditions (*Re*), a systematic methodology introduced by [8, 9] for the design and optimization of microdevices, is employed. It is a CFD-based optimization method where CFD is coupled with an optimization strategy based on the use of Design of Experiments (DOE), Surrogate Modelling (SM) and Multi-Objective Genetic Algorithm (MOGA) techniques. The optimization process starts with the definition of the design parameters to be evaluated and their range of variation (design space) in the study and the performance criteria or parameters to be controlled (maximized or minimized). The DOE explores the space of design parameters and provides a table of sampling designs which are then evaluated by numerical simulation (CFD) to obtain the corresponding performance parameters. The design and performance parameters are used by the SM technique to create the approximate correlate functions (response surfaces). Then, the design and performance parameters values are correlated in approximate functions (objective functions or response surfaces) developed by the SM technique. Eventually, the MOGA is applied on the response surfaces to find the Pareto front (Pf) of designs that give the trade-off of the performance parameters to achieve the optimization goal, where the best

compromise of the performance parameters can be chosen to fulfil the design requirements. CFD simulations are carried out to evaluate the accuracy of values of performance parameters predicted in the Pareto front.

In this study, the difference $\varsigma_- - \varsigma_+$ and the sum $\varsigma_- + \varsigma_+$ of the pressure drop coefficients in the diverging (ς_+) and converging (ς_-) directions are made the performance parameters. The Pressure drop coefficient ς is calculated by equation (1) given in section 1.

The models of the diffuser/nozzle in the study are defined on the basis of the geometric or design parameters shown in figure 1. The design parameters selected for optimization are shown in Table 1.

The DOE technique used to define the original set of sample models is the Optimal Latin Hypercube (OLH) [15]. OLH uses the same number of levels for each design parameter than the number of experiments (configurations or design points) with a combination optimized to evenly spread the design points within *n*-dimensional space defined by *n* design parameters, $n = 4$ in this study. The number of experiments (designs points) and levels of design parameters in this study is 31. In these models, the performance parameters are evaluated by numerical simulations (CFD). The correlation of the design and performance parameters is obtained by the surrogate model Radial Basis Function (RBF) [16-18]. Finally, the Non-dominated Sorting Genetic Algorithm (NSGA-II) [19] is applied on the response surfaces with the optimization goal of maximizing $\zeta_- - \zeta_+$ and minimizing $\zeta_- + \zeta_+$ to find the optimum cases in a Pareto front (Pf) that gives the trade-off of $\zeta_- - \zeta_+$ and $\zeta_- + \zeta_{+,}$ the following values of parameters of the genetic algorithm were used after testing its effectiveness: Population size = 32, Number of generations = 100, Crossover probability = 0.9, Crossover distribution index = 20 and Mutation distribution index = 100.

3. Numerical simulation

Numerical simulations of the transport process are performed to investigate the rectification efficiency obtained for different *Re* numbers in the diffuser/nozzle model geometries defined by the DOE. For each Re and each model, one simulation is made on the nozzle direction and one on the diffuser direction. The CFD code used for this study is the commercial Navier-Stokes Solver CFX-11 [20] which is based on the Finite Volume Method. The geometries of the diffuser/nozzle models were constructed and meshed by using the commercial mesh generator CFX-Mesh [20].

The flow is defined viscous, isothermal, incompressible, laminar and in steady-state, for which continuity equation (2), and momentum equation (3) are solved.

$$\nabla.\vec{V} = 0 \tag{2}$$

$$\rho\vec{V}\nabla\vec{V} = -\nabla P + \mu\nabla^2\vec{V} \tag{3}$$

where ρ and μ are the density and viscosity of the fluid respectively, $\vec{V}$ and P are the velocity vector and pressure, respectively. Advection terms in each equation are discretized with a second order differencing scheme which minimize numerical diffusion in the results. The simulations were defined to reach convergence when the normalized residual for the mass fraction fell below 1 x 10^{-5}.

The boundary condition of the velocity at the inlet section is mass inflow so that only the component in the direction of bulk flow exists to have a uniform velocity profile and the other components are zero. The velocity value at the inlet depends on the geometry and the Reynolds number (*Re*) to have in the inlet channel. The study has been made for *Re* in 100-1000 with increments of 100. Along the walls, non-slip boundary condition is used for the tangential velocity component whereas the normal component is zero. At the outlet end of the mixing channel, a constant pressure condition (gauge pressure $P = 0$) is specified on an opening section. Water at 25ºC is the fluid used in this study. Flow vector fields and pressure contours from the simulations results are examined to ensure that the boundary conditions are fulfilled.

A variable mesh is used, which is composed of triangular elements extruded from one surface to the opposite one to form 10 layers of wedge cells and prism cells located adjacent to walls and arranged to provide sufficient resolution for boundary layers near the fluid-solid interface on the walls of the channels. The number of mesh cells in the models is in the order of 1 million. In order to obtain mesh-independent results from the simulations, a preliminary mesh size sensitivity study was carried out to determine the interval size of convergence.

4 RESULTS AND ANALYSIS

Based on the methodology used in this study, the design and optimization tools (CFD, RBF, MOGA) in the procedure are applied for 10 different Reynolds numbers (100 to 1000 in increments of 100). The results can be categorised in two sections. In the first section the acquired results from CFD analysis are discussed and in the second section the optimisation results are validated with CFD analysis and discussed in more detail.

4.1 CFD Study

In total 620 simulations are done (62 for each Reynolds number) which half of them are done for diffuser direction and the other half for the nozzle direction. There are some interesting trends that can be seen based on this study. $\varsigma_- - \varsigma_+$ versus Reynolds number for first 10 cases (Table 2) given by OLH is shown in Figure 2-a. As it can be seen in this figure case 4 shows the highest average $\varsigma_- - \varsigma_+$ value for this range of Reynolds number, therefore this design can produce higher pressure rise than other 9 cases in the operating range of 100<Re<1000. Figure 3-a shows $(\varsigma_- - \varsigma_+)/(\varsigma_- + \varsigma_+)$ which is a measure of net volume flow rate [2] versus Reynolds number. As it is depicted $(\varsigma_- - \varsigma_+)/(\varsigma_- + \varsigma_+)$ increases as Re increases in all cases, but this raise is more dramatic for cases 5 and 7. Therefore, cases 5 and 7 can be better designs to results in higher flow rates (higher rectification efficiency). As explained earlier the Reynolds number in Figure 2-a and Figure 3-a is based on the hydraulic diameter of inlet channel. It would be more useful to have the data based on throat Reynolds number. Figure 2-b and Figure 3-b show $\varsigma_- - \varsigma_+$ and

$(\varsigma_- - \varsigma_+)/(\varsigma_- + \varsigma_+)$ versus throat Reynolds number, respectively.

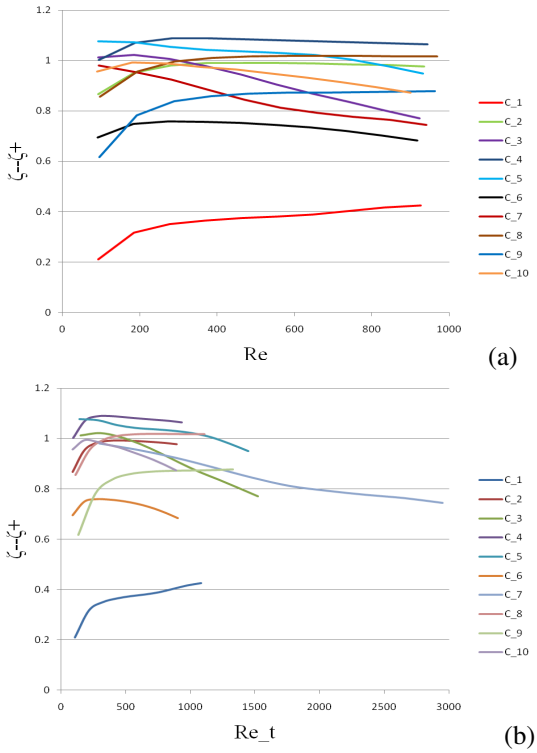

Figure 2. $(\varsigma_- - \varsigma_+)$ which is a measure of maximum pressure that pump can withstand is shown against *Re* and throat *Re* (*Re_t*) in (a) and (b) respectively

The trend in Figure 2-b and Figure 3-b is similar to Figure 2-a and Figure 3-a, respectively. As it is expected the throat Reynolds number is higher for designs with narrower throat (such as case 7). Figure 4 shows velocity and pressure contours for case 5 for Re=500 for both diffuser and nozzle directions. Lots of data can be extracted from these 620 simulations. To make this part brief only some of these results are presented. Here we present variation of $\varsigma_- - \varsigma_+$ against one of geometrical variables (*W2*)as it is of more interest of research studies (Figure 5).

It can be concluded that CFD results give us a good insight for the best design among simulated cases but it cannot easily identify the optimum design for the considered parameter ranges. Here, significant amount of computational time is spent to obtain the results for only 31 different designs which show that the optimisation algorithm should be implemented to identify the optimum design more effectively in a limited time. It should be noted that these are steady state simulations and cannot capture the unsteady behaviour of diffuser/nozzle elements in valveless micropumps, but they can be a good indication of performance of these elements in pumps which operate in quasi-steady regime i.e. Wo < 0.5 [21].

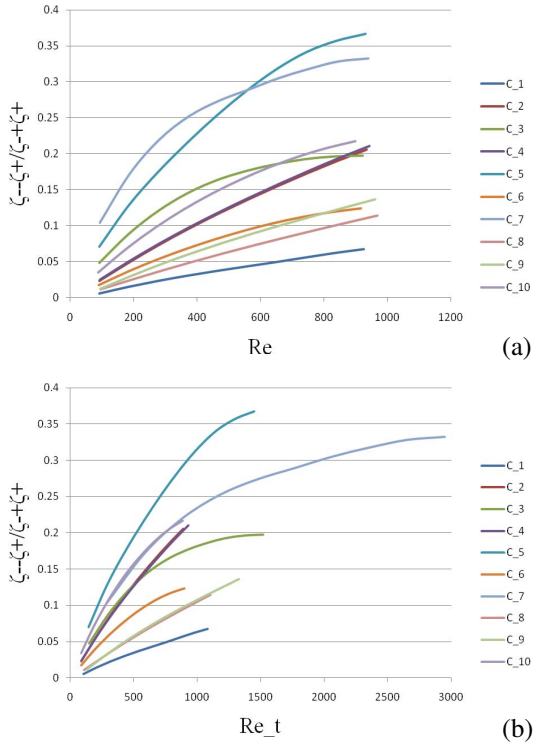

Figure 3. $(\varsigma_- - \varsigma_+)/(\varsigma_- + \varsigma_+)$ which is a measure of maximum volume flow rate of a micropump is shown against *Re* and throat *Re* (*Re_t*) in (a) and (b) respectively

4.2 Optimisation

As explained earlier CFD results are used as the basis of the optimisation procedure. To validate the results from optimisation algorithm six cases from Pf are simulated to see the correlation between prediction (from optimisation algorithm) and CFD results. This comparison for *Re*=200 is shown in Figure 6. As one can see, the agreement between prediction and CFD results is acceptable. To see the pattern clearer normalised prediction and CFD results are shown in Figure 7.

Table 2. Ten first cases out of 31 cases under study

	W1(μm)	W2(μm)	D(μm)	r(μm)
C_1	1503	1966	360	831
C_2	1945	5028	314	859
C_3	952	2069	376	514
C_4	1890	5365	267	638
C_5	1062	5062	329	583
C_6	1834	2821	407	569
C_7	400	1779	283	652
C_8	1669	3572	143	555
C_9	1338	2979	174	886
C_10	1779	3552	500	762

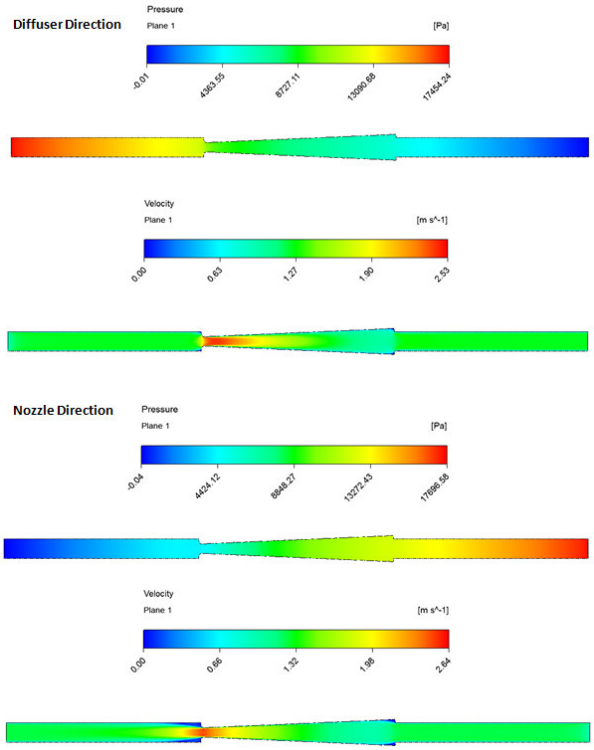

Figure 4. Pressure and velocity contours for case 5 and Re=500 for both diffuser and nozzle directions.

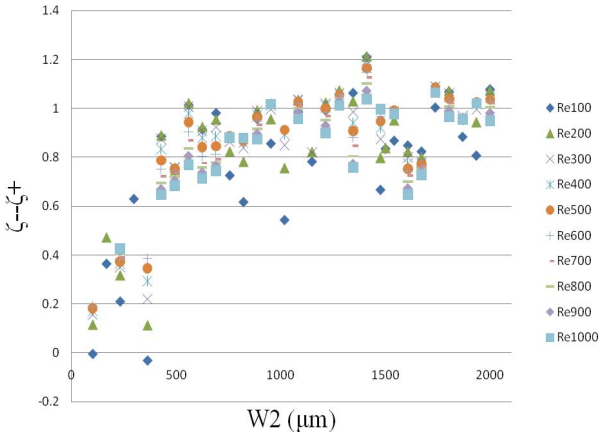

Figure 5. Variation of $\varsigma_- - \varsigma_+$ with *W2:* The trend that as *W2* increases $\varsigma_- - \varsigma_+$ increases can be observed**.**

The prediction and CFD results are reasonably close and this confirms that this methodology works efficiently and can reduce the design time dramatically.

From the Pf curves shown in Figures 6 and 7 the designer can identity the geometries of diffuser/nozzle element that corresponds to the desirable levels flow rate and pressure rise for a particular application. Each node in the Pf corresponds to a specific geometry of the element where the influence of the design parameters on the performance parameters ($\varsigma_- - \varsigma_+$ and $\varsigma_- + \varsigma_+$) can also be investigated at different *Re* numbers.

One interesting observation is that optimized geometries are different for different *Re* numbers. This implies that further study is necessary to investigate the behavior of these rectifying elements under different flow conditions (*Re*, unsteady regimes).

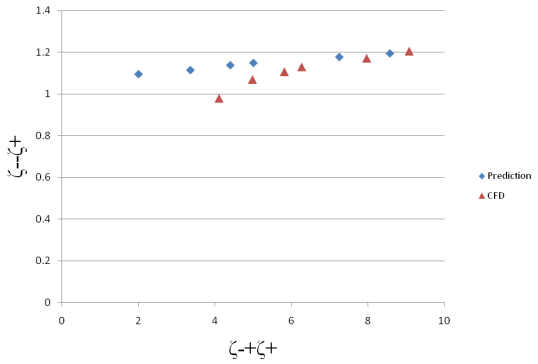

Figure 6. $\varsigma_- - \varsigma_+$ versus $\varsigma_- + \varsigma_+$ in six selected designs of the Pareto Front from optimization on RBF approximation surfaces (Re=200).

5 CONCLUSIONS

A systematic evaluation has been made on flow, pressure drop and rectification property of a diffuser/nozzle element under quasi-steady conditions for a valveless micropump. The geometries defined by four geometric parameters provide different flow characteristics for the diffuser/nozzle element and consequently in a valveless micropump, resulting in enhanced performance. This parametric control, which covers continues ranges of the design parameters, is only possible with the use of a systematic design and optimization methodology where CFD is integrated within a numerical optimization strategy. The results show that it is possible to predict the trend of the two performance parameters, $\zeta_- - \zeta_+$ and $\zeta_- + \zeta_{+,}$ for different designs of the diffuser/nozzle element in order to maximise pressure rise and flow rate.

ACKNOWLEDGMENTS

We gratefully acknowledge financial support from Engineering and Physical Sciences Research Council (EPSRC) through the Dorothy Hodgkin Postgraduate Award (DHPA). We also thank Prof. Mehrdad Zangeneh for his support with computational resources.

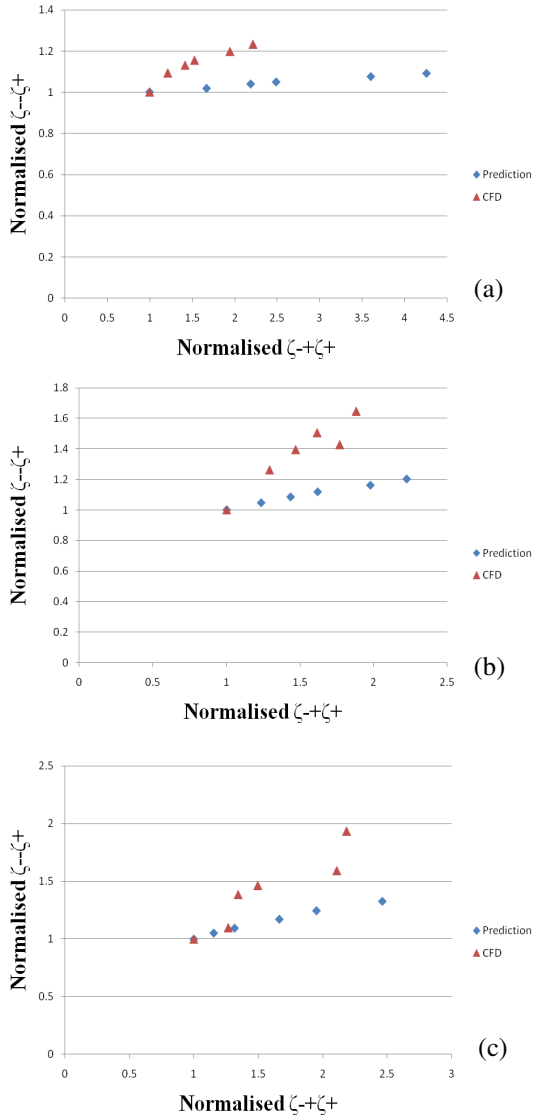

Figure 7. Normalized $\varsigma_- - \varsigma_+$ versus normalized $\varsigma_- + \varsigma_+$ in six selected designs of the Pareto Front from optimization on RBF approximation surfaces ((a) Re=200, (b) Re=700 and (c) Re=1000).

REFERENCES

1. E. Stemme and G. Stemme, *A valveless diffuser/nozzle-based fluid pump.* Sensors and Actuators A: Physical, 1993. **39**(2): p. 159-167.
2. I. Eames, A. Azarbadegan, and M. Zangeneh, *Analytical model of valveless micropumps.* Journal of microelectromechanical systems, 2009. **18**(4): p. 878-883.
3. A. Olsson, G. Stemme, and E. Stemme, *A valve-less planar fluid pump with two pump chambers.* Sensors & Actuators: A. Physical, 1995. **47**(1-3): p. 549-556.
4. T. Gerlach and H. Wurmus, *Working principle and performance of the dynamic micropump.* Sensors & Actuators: A. Physical, 1995. **50**(1-2): p. 135-140.
5. R.L. Bardell, et al., *Designing high-performance micro-pumps based on no-moving-parts valves.* ASME-PUBLICATIONS-HTD, 1997. **354**: p. 47-54.
6. F.K. Forster, et al., *Design, fabrication and testing of fixed-valve micro-pumps.* ASME-PUBLICATIONS-FED, 1995. **234**: p. 39-44.
7. S. Matsumoto, A. Klein, and R. Maeda. *Development of bi-directional valve-less micropump for liquid.* 1999.
8. C.A. Cortes-Quiroz, M. Zangeneh, and A. Goto, *On multi-objective optimization of geometry of staggered herringbone micromixer.* Microfluidics and Nanofluidics, 2009. **7**(1): p. 29-43.
9. C.A. Cortes-Quiroz, M. Zangeneh, and A. Goto. *A Multi-Objective Analysis and Optimization Methodology for the Design of Passive Micromixers Based on Their Own Topology*. 2008.
10. A. Azarbadegan, E. Moeendarbary, C.A. Cortes-Quiroz, and I. Eames, *Investigation of Double-Chamber Series Valveless Micropump: An Analytical Approach.* 2010.
11. Y.C. Wang, J.C. Hsu, P.C. Kuo, and Y.C. Lee, *Loss characteristics and flow rectification property of diffuser valves for micropump applications.* International Journal of Heat and Mass Transfer, 2009. **52**(1-2): p. 328-336.
12. A. Olsson, G. Stemme, and E. Stemme, *Numerical and experimental studies of flat-walled diffuser elements for valve-less micropumps.* Sensors and Actuators A: Physical, 2000. **84**(1-2): p. 165-175.
13. A. Azarbadegan, C.A. Cortes-Quiroz, I. Eames, and M. Zangeneh, *Analysis of double-chamber parallel valveless micropumps.* Microfluidics and Nanofluidics, 2009: p. 1-10.
14. C.A. Cortes-Quiroz, A. Azarbadegan, and E. Moeendarbary, *An efficient passive planar micromixer with fin-shaped baffles in the tee channel for wide Reynolds number flow range.* Proceedings of World Academy of Science, Engineering and Technology, 2010. **61**: p. 170-175.
15. K.Q. Ye, W. Li, and A. Sudjianto, *Algorithmic construction of optimal symmetric Latin hypercube designs.* Journal of statistical planning and inference, 2000. **90**(1): p. 145-159.
16. R.L. Hardy, *Multiquadric equations of topography and other irregular surfaces.* J. Geophys. res, 1971. **76**(8): p. 1905-1915.
17. E.J. Kansa, *Multiquadrics--A scattered data approximation scheme with applications to computational fluid-dynamics--I surface approximations and partial derivative estimates.* Computers & mathematics with applications, 1990. **19**(8-9): p. 127-145.
18. R.L. Hardy, *Theory and applications of the multiquadric-biharmonic method. 20 years of discovery 1968-1988.* Computers & Mathematics with Applications, 1990. **19**(8): p. 163-208.
19. K. Deb, A. Pratap, S. Agarwal, and T. Meyarivan, *A Fast Elitist Multi-Objective Genetic Algorithm: NSGA-II.* IEEE Transactions on Evolutionary Computation, 2000. **6**: p. 182-197.
20. ANSYS, *EuropeLtd. CFX 11.0 User Manual.* 2007.

21. C.L. Sun and K.H. Huang, *Numerical characterization of the flow rectification of dynamic microdiffusers.* Journal of Micromechanics and Microengineering, 2006. **16**: p. 1331-1339.